Original Research Article

J. Funct. Mater. Biomol. 1(2)-2017 pp 57-63

SACRED HEART RESEARCH PUBLICATIONS

Journal of Functional Materials and Biomolecules

Journal homepage: www.shcpub.edu.in

ISSN: 2456-9429

Phase relations and thermodynamics in the system GaSe–GaS–GaTe

MirSalim M. Asadov*, Asif N. Mammadov, Dilgam B. Tagiyev

Received on 01 Jan 2017, Accepted on 13 Sep 2017

Abstract

The system GaSe–GaS–GaTe was investigated and the *T*–*x* phase diagram of GaSe–GaS studied in detail by differential thermal analysis, X-ray diffractometry and thermodynamically calculations. We clarify the temperature and melting enthalpy of the components that are needed to calculate thermodynamic parameters of GaSe–GaS system. In view of isothermal sections system is significantly affected by the phase boundary of the formation of solid solutions in the systems. Built isothermal section of GaSe–GaS–GaTe system at 298 K and four phases of solid solutions (based on GaSe, on GaS, on GaTe and on Ga_2SeTe) were found.

Keywords: phase relations, thermodynamics, gallium monochalcogenides

1 Introduction

Gallium monochalcogenides (GaX, X–S, Se, Te) are layered compounds like graphite that can be readily reduced to two-dimensional (2D) form due to their strong in-plane bonding and weak interlayer van der Waals coupling. It is known that GaX form complex composition solid solutions. Gallium monoselenide (β–, ε–, γ– and δ–GaSe) has several polymorphs. Data on the crystal and electron structure of GaX (X–S, Se, Te) type compounds are shown in [1]. The thermodynamically most stable modification is ε– GaSe, which belongs to hexagonal syngony, is characterized by a layered structure and space group $D_{3h}^{1} - P\overline{6}_{3}m2$ [1]. Layered crystals of type GaX have anisotropic properties, which are caused by the presence of two kinds of bonds between atoms in the crystal [2]. Each layer, e.g. GaSe, contains four atomic planes Se-Ga-Ga-Se perpendicular to the *c*-axis of hexagonal crystal. Bond is ionic-covalent inside the layers, and neighboring layers are bound by weak forces such as van der Waals forces. GaSe and GaS (space group $D_{6h}^{4} - P\overline{6}_{3}/mmc$ or β-type GaS) are wide-gap semiconductors and at room temperature have a band gap at around 1.98 and 2.53 eV, respectively. GaSe because of its unique properties can be used in various fields of science and technology. The wide-gap GaX semiconductor materials have several advantages over other materials: a larger area of operating temperatures, the ability to create on their basis light-emitting devices in the visible spectrum, high values of the critical field of electrical breakdown, radiation resistance [3,4].

GaSe-based materials have low hardness, mechanical strength and susceptible to micro-delamination. To eliminate these drawbacks, it is important to modify the properties of crystals, e.g. by doping or producing GaX–based solid solutions. However, with increasing hardness of crystals it is also necessary to maintain high optical properties and nonlinear susceptibility. Taking into account the practical application of GaX-based materials makes it relevant to establish the concentration dependences of the properties of the samples of GaSe–GaS–GaTe system. A survey of known phases in the system GaSe–GaS–GaTe is given in [5]. Physicochemical interactions in the GaS–GaSe–GaTe system were studied by differential thermal analysis X-ray powder diffraction, and microhardness measurements. The GaSe–GaS–GaTe system is triangulated into two ternary subsystems. An isothermal section of this system presented in [5] shows four areas of solid solutions based on binary chalcogenides of gallium and intermediate phase Ga_2SeTe. Thus the aim of this study was to clarify the phase diagram of GaSe–GaS–GaTe quasi-ternary system, determination of the concentration dependences of physico-chemical properties of the $GaSe_{1-x}S_x$ crystals.

2 Experimental and theoritical techniques

2.1. Material preparation and experimental details

Ga-5N gallium, B5 sulfur, and OSCh-17-3 selenium with impurity content no higher than 5 × 10^{-4} wt % were used in the synthesis of GaS and GaSe compounds. The synthesis was performed by melting starting elements taken in stoichiometric ratios in evacuated (pressure of 10^{-3} Pa) and sealed quartz ampules. The ampules were held for 6–8 h at a temperature higher than the liquidus temperature by 25–30 K (melting points of GaS and GaSe are 1288 and 1211 K, respectively) and then allowed to cool to room temperature. The prepared compounds GaS and GaSe were identified by DTA (a heating/cooling rate of 10 K/min) and powder X-ray diffraction analysis using the literature data for comparison. Solid solutions $GaSe_{0.8}\,S_{0.2}$

---

* Corresponding author: e-mail mirasadov@gmail.com,
Nagiyev Institute of Catalysis and Inorganic Chemistry, Azerbaijan National Academy of Sciences, av. H. Javid 113, Baku, AZ1143 Azerbaijan

were prepared analogously by melting stoichiometric weighed portions of preliminarily prepared starting GaS and GaSe components in evacuated quartz ampoules.

Single crystals of GaSe and $GaSe_{0.8}S_{0.2}$ solid solutions were grown by the Bridgman–Stockbarger method. Polycrystalline samples of the prepared compounds and solid solutions of specified compositions were ground and loaded into separate quartz ampules 8- to 10-cm-long with an inner diameter of 1 cm and sharpened ends. A quartz ampule with a sample was placed in the dual-zone furnace of a device for single crystal growth. In the course of crystal growth from a melt, the temperature of 1293 K (5 K higher than the melting point of GaS) was maintained in the upper zone of the furnace and the temperature of 1200 K (10 K lower than the melting point of GaSe) was maintained in the lower zone. The ampule was moved in the furnace at a rate of 0.3–0.5 cm/h, and the temperature gradient near the crystallization front was 25 ± 3 K. The abovementioned rate of movement of the ampule with a sample in the furnace was optimal for the growth of a nucleus of a single crystal. In other words during the preparation of GaSe-GaS single crystals by method of directional solidification the melt cooling rate was selected to ensure the crystallization front close to the flat. Due to concentration supercooling during $GaSe_{0.8}S_{0.2}$ growth at speeds > 0.5 cm/h there is loss of morphological stability of a flat front and transition to the cell structure [6].

The X-ray diffraction studies of the GaX and $GaSe_{0.8}S_{0.2}$ solid solutions were performed on a D2PHASER-ray diffractometer using monochromatic Cu*Kα* radiation (Ni-filter). A single-crystal graphite plate used as a monochromator was placed in the path of a reflected beam. For example, for GaSe lattice parameters are: a = 3.755 ± 0.002 Å and c = 15.940 ± 0.005Å at room temperature. The GaSe crystals belong to the space group $P\bar{6}m$ and cleave readily along the (0001) plane.

2.2. Calculation of the phase diagram for GaSe-GaS

T– x phase diagrams of binary and multinary systems make it possible to critically examine existing schemes and to identify new ways to improve the manufacturing processes. We calculated T (x) dependences of the GaSe-GaS system at constant (atmospheric) pressure, not taking into account the molecular states of chalcogens in gas phase and compared calculation results with experiment. These calculations help optimize technological parameters of crystal formation processes, in particular, to establish the temperature of melt and solid phase appearance. Practice shows that it is impossible to uncontrollably raise the temperature in systems containing gallium chalcogenides because at temperatures above melting point of GaX, ampoules may be destroyed due to high vapor pressure of chalcogens.

GaSe–GaS is the example of isomorphous system. The complete solubility in GaSe-GaS occurs because both GaSe and GaS have the same crystal structure, Se and S have similar radii, electronegativity and valence. In GaSe-GaS system melting occurs over a narrow temperature range, between the solidus and liquidus lines. Solid and liquid phases are at equilibrium in this temperature range.

In particular, T–x phase diagram of GaSe–GaS, is a graphical representation of the equilibrium state of a system using the intensive variables T and x_1 while p is kept constant. However, in the process of single crystal growth in this GaSe–GaS system vapor pressure of components is higher than the liquidus temperature of the components and is greatly increasing with increasing temperature. Therefore, the calculation of the liquidus and solidus line of the phase diagram of GaSe–GaS has a practical importance. The equilibrium may be calculated from thermodynamic data using Gibbs energies for all relevant phases. For calculation of the T–x phase diagram for GaSe–GaS, we used a method comprising ratios between the concentrations of initial components and their thermodynamic enthalpies of melting [7, 8]. Thus the liquidus and solidus lines of the binary system 1–2 with continuous rows of liquid and solid solutions can be analytically described by the formulae

$$x_1^l = \frac{1-F_2}{F_1-F_2},$$

$$x_1^s = F_1 x_1^l$$

$$F_i = \exp\left[\frac{\Delta H_i^{0,m}\left(T^{-1}-T_i^{-1,m}\right)}{R}\right] \qquad (1)$$

x_i^l and x_i^s are the mole fractions of the compound in the equilibrium liquid and solid solutions, respectively, x_i^l and T_i^m and $\Delta H_i^{0,m}$ - the melting temperature and melting enthalpy of the i^{th} component, R- universal gas constant. To build T-x phase diagram for GaSe-GaS, for each particular T_i^m, F_1 and F_2 values were calculated and then via formula (5) x_1^l and x_1^s values were found.

The melting temperature and melting enthalpy of GaSe and GaS were determined by melting peak areas measured according to the DTA. Al_2O_3 was the standard compound. The rate of heating (cooling) of the samples was 10 K/min. Weights of batches are 0.3 g. The values of GaSe and GaS specific melting enthalpies were determined according to the following formula: $\Delta H_i^m = \left(\Delta H_{st}^m \cdot S_i \cdot T_i^m\right) / \left(S_{st} \cdot T_{st}^m\right)$, where ΔH_{st}^m is the specific enthalpy of melting of standard compound; S_i, S_{st} are peak areas of differential curves of melting of component and the standard compound respectively; T_{st}^m is the melting temperature of the standard compound. To carry out calculations based on DTA data for GaSe and GaS the following melting parameters of components were chosen: ΔH_i^m (GaSe)= 30300 J/mol, T^m (GaSe)= 1211 K, ΔH_i^m (GaS)= 34800 J/mol, and T^m (GaS)= 1288 K. The calculation results lines Single crystals of GaSe and $GaSe_{0.8}S_{0.2}$ solid solutions were grown by the Bridgman–Stockbarger method. Polycrystalline samples of the prepared compounds and solid solutions of specified compositions were ground and loaded into separate quartz ampules 8- to 10-cm-long with an inner diameter of 1 cm and sharpened ends. A quartz ampule with a sample was placed in the dual-zone furnace of a device for single crystal growth. In the course of crystal growth from a melt, the temperature of 1293 K (5 K higher than the melting point of GaS) was maintained in the upper zone of the furnace and the temperature of 1200 K (10 K lower than the melting point of GaSe) was maintained in the lower zone. The ampule was moved in the furnace at a rate of 0.3–0.5 cm/h, and the temperature gradient near the crystallization front was 25 ± 3 K. The abovementioned rate of movement of the ampule with a sample in the furnace was optimal for the growth of a nucleus of a single crystal. In other words during the preparation of GaSe-GaS single crystals by method of directional solidification the melt cooling rate was selected to ensure the crystallization front close to the flat. Due to concentration supercooling during $GaSe_{0.8}S_{0.2}$ growth at speeds > 0.5 cm/h there is loss of morphological stability of a flat front and transition to the cell structure [6].

The X-ray diffraction studies of the GaX and $GaSe_{0.8}S_{0.2}$ solid solutions were performed on a D2PHASER-ray diffractometer using monochromatic Cu*K*α radiation (Ni-filter). A single-crystal graphite plate used as a monochromator was placed in the path of a reflected beam. For example, for GaSe lattice parameters are: *a* = 3.755 ± 0.002 Å and *c* = 15.940 ± 0.005Å at room temperature. The GaSe crystals belong to the space group $P\bar{6}m$ and cleave readily along the (0001) plane.

2.2. Calculation of the phase diagram for GaSe-GaS

T– *x* phase diagrams of binary and multinary systems make it possible to critically examine existing schemes and to identify new ways to improve the manufacturing processes. We calculated T (*x*) dependences of the GaSe-GaS system at constant (atmospheric) pressure, not taking into account the molecular states of chalcogens in gas phase and compared calculation results with experiment. These calculations help optimize technological parameters of crystal formation processes, in particular, to establish the temperature of melt and solid phase appearance. Practice shows that it is impossible to uncontrollably raise the temperature in systems containing gallium chalcogenides because at temperatures above melting point of GaX, ampoules may be destroyed due to high vapor pressure of chalcogens.

GaSe–GaS is the example of isomorphous system. The complete solubility in GaSe-GaS occurs because both GaSe and GaS have the same crystal structure, Se and S have similar radii, electronegativity and valence. In GaSe-GaS system melting occurs over a narrow temperature range, between the solidus and liquidus lines. Solid and liquid phases are at equilibrium in this temperature range.

In particular, T–*x* phase diagram of GaSe–GaS, is a graphical representation of the equilibrium state of a system using the intensive variables T and x_1 while *p* is kept constant. However, in the process of single crystal growth in this GaSe–GaS system vapor pressure of components is higher than the liquidus temperature of the components and is greatly increasing with increasing temperature. Therefore, the calculation of the liquidus and solidus line of the phase diagram of GaSe–GaS has a practical importance. The equilibrium may be calculated from thermodynamic data using Gibbs energies for all relevant phases. For calculation of the T–*x* phase diagram for GaSe–GaS, we used a method comprising ratios between the concentrations of initial components and their thermodynamic enthalpies of melting [7, 8]. Thus the liquidus and solidus lines of the binary system 1–2 with continuous rows of liquid and solid solutions can be analytically described by the formulae

$$x_1^l = \frac{1 - F_2}{F_1 - F_2},$$

$$x_1^s = F_1 x_1^l$$

$$F_i = \exp\left[\frac{\Delta H_i^{0,m}\left(T^{-1} - T_i^{-1,m}\right)}{R}\right] \qquad (1)$$

x_i^l and x_i^s are the mole fractions of the compound in the equilibrium liquid and solid solutions, respectively, x_i^l and T_i^m and $\Delta H_i^{0,m}$ - the melting temperature and melting enthalpy of the i^{th} component, *R*- universal gas constant. To build T-*x* phase diagram for GaSe-GaS, for each particular T_i^m , F_1 and F_2 values were calculated and then via formula (5) x_1^l and x_1^s values were found.

The melting temperature and melting enthalpy of GaSe and GaS were determined by melting peak areas measured according to the DTA. Al_2O_3 was the standard compound. The rate of heating (cooling) of the samples was 10 K/min. Weights of batches are 0.3 g. The values of GaSe and GaS specific melting enthalpies were determined according to the following formula: $\Delta H_i^m = \left(\Delta H_{st}^m \cdot S_i \cdot T_i^m\right) / \left(S_{st} \cdot T_{st}^m\right)$, where ΔH_{st}^m is the specific enthalpy of melting of standard compound; S_i, S_{st} are peak areas of differential curves of melting of component and the standard compound respectively; T_{st}^m is the melting temperature of the standard compound. To carry out calculations based on DTA data for GaSe and GaS the following melting parameters of components were chosen: ΔH_i^m (GaSe)= 30300 J/mol, T^m (GaSe)= 1211 К, ΔH_i^m (GaS)= 34800 J/mol, and T^m (GaS)= 1288 К. The calculation results lines liquidus (T^m) and solidus (T^s) of the system GaSe–GaS are shown in Table.

$\Delta_f G_T^0(x,T)$ data are important for modeling the materials preparation process and investigating solid-liquid transitions at varied component concentrations. $\Delta_f G_T^0(x,T)$ composition and temperature dependences for $GaSe_{1-x}S_x$ solid solutions were calculated using a modified solution model which included nonmolecular compounds [9].

For the Gibbs free energy of formation of $GaSe_{1-x}S_x$ solid solutions from their constituent elements at *p*,*T*=const, we obtained the Eq. 2

$$\begin{aligned}&\Delta_f G_T^0(\mathrm{J/mol}) = (1-x)\Delta_f H_{298.15}^0(\mathrm{GaSe}) + \\ &+ x\Delta_f H_{298.15}^0(\mathrm{GaS}) - (1-x)T\Delta_f S_{298.15}^0(\mathrm{GaSe}) - \\ &- x\Delta_f S_{298.15}^0(\mathrm{GaS}) - T\Delta C_{p,298.15}^0 \times \\ &\times\left[\ln\left(\frac{T}{298.15}\right) + \left(\frac{298.5}{T}\right) - 1\right] + \\ &+ RT[(1-x)\ln(1-x) + x\ln x] + \Delta_f G_T^{o,ex}\end{aligned} \qquad (2)$$

where x is the mole fraction of GaS; 1–*x* is the mole fraction of GaSe; $\Delta_f H_{298.15}^0$ and $\Delta_f S_{298.15}^0$ are the enthalpy and entropy of formation of the compounds GaSe and GaS; $\Delta C_{p,298.15}^0$ is the difference between the heat capacities of the $GaSe_{1\text{-}x}S_x$ solid solutions and the compounds GaSe and GaS, respectively; and $\Delta_f G_T^{0,ex}$ is the excess molar Gibbs free energy of mixing.

Table. The calculation results on lines liquidus and solidus of the system GaSe-GaS

The composition, mole fraction GaS	Liquidus, T^s (K)	Solidus, T^l (K)
0	1238	1238
0.05	1223	1234
0.1	1211	1228
0.15	1204	1222
0.2	1199	1216
0.25	1196	1207
0.3	1194	1197
0.32	1193	1193
0.4	1194	1204
0.5	1197	1217
0.6	1202	1230
0.7	1212	1245
0.8	1229	1260
0.9	1254	1275

3 Results and Discussion

3.1. T-*x* phase diagram of GaSe-GaS

Phase diagram for GaSe-GaS system has been studied by various authors before. Version of T-*x* phase diagram of GaSe-GaS proposed by Rustamov *et al.* [5] has not been confirmed by our follow-up research. In [5] shows melting points 1233 and 1238 K for initial GaSe and GaS respectively. Therefore, a known T–*x* phase diagram for GaSe-GaS requires adjustment.

Our calculation results for liquidus and solidus lines of GaSe-GaS system were compared with data from the corresponding literature [5]. For calculation of T–*x* phase diagram for GaSe–GaS we used aforementioned technique [7, 8], taking into account temperatures and enthalpies of melting of initial components [10–13].

Our studied and calculated phase diagram for GaSe-GaS is shown in Fig.1. Calculated solidus and liquidus temperatures (Table) differ slightly from the experimental data (difference the solidus was ~5 K and a liquidus - ~15 K).

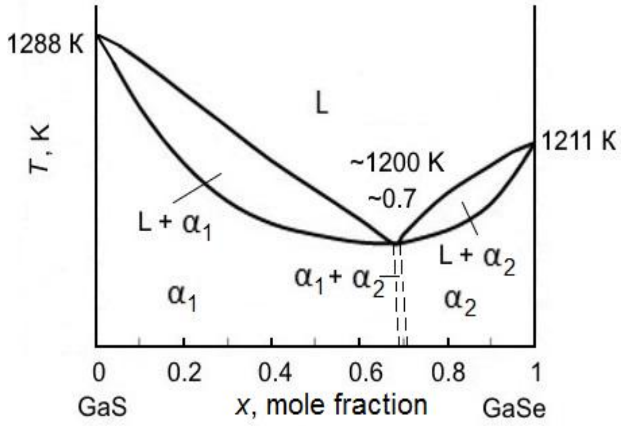

Fig. 1. T-*x* phase diagram of the GaSe-GaS system calculated and constructed by us.

Diagram of the state for GaSe-GaS system is the type characterized by the minimum (30 mol.% GaS and 1200 K) and presence of unlimited mutual solubility in the system. This is due to the proximity of the crystal structure source components. The different phases are not detected in the area of $GaSe_{1\text{-}x}S_x$ solid solutions. This is consistent with thermodynamic calculations of the free energy of mixing [9] of $GaSe_{1\text{-}x}S_x$ solid solutions. Calculation of the temperature dependence of the free energy of mixing of solid solutions was performed in 300-1200 K range.

3.2.1. Thermodynamics of the GaSe-GaS system

The $\Delta_f G_T^0(x,T)$ dependences of $GaSe_{1\text{-}x}S_x$ were calculated by Eq. (2). In equation (2), the last two terms are the free energy of mixing in the formation $GaSe_{1\text{-}x}S_x$ of GaSe and GaS.

To this end, we used the thermodynamic functions of the GaSe and GaS compounds:

$\Delta_f H_{298.15}^0(\mathrm{GaS}) = \text{-}194650 \pm 14650\ \mathrm{J/mol}$,

$\Delta_f S_{298.15}^0(\mathrm{GaS}) = \text{-}\,420 \pm 290\ \mathrm{J/(mol\ K)}\,[10]$

and $\Delta_f H_{298.15}^0(\mathrm{GaSe}) = \text{-}159000\ \mathrm{J/mol}\,[13]$ $\Delta_f S_{298.15}^0(\mathrm{GaSe}) = \text{-}11\ \mathrm{J/(mol\ K)}$. With allowance for the heat capacity of the binary compounds GaS $\left(C_{p,298.15}^0 \approx 47\ \mathrm{J/mol\ K}\right)$ and GaSe ($C_{p,298.15}^0 \approx 48\ \mathrm{J/mol\ K}$), the composition dependences of the room temperature heat capacity, $\Delta C_{p,298.15}^0(x)$, for the $GaSe_{1\text{-}x}S_x$ solid solutions were calculated. The partial excess molar Gibbs free energy $\Delta_f \overline{G}_T^{0,ex}$ of the GaSe and GaS compounds was calculated using the phase diagram of the GaSe–GaS system. The values $\Delta_f \overline{G}_T^{0,ex}$ of the GaX were evaluated as [9]

$$\Delta_f G_T^{0,ex} = T\left[\Delta S_i^m - R\ln\left(x_i^l / x_i^s\right)\right] - \Delta H_i^m \quad (3)$$

where T is a temperature on the solidus line; the subscript refers to the GaSe (or GaS) compound. The corresponding parameters were defined by the formula: $\Delta S^m = \Delta H^m / T^m$, $\Delta S^m(\text{GaSe}) \approx 25.4$ J/(mol K) and $\Delta S^m(\text{GaS}) \approx 27.3$ J/(mol K).

Using the calculated partial values $\Delta_f \overline{G}_T^{0,ex}$ of the GaSe and GaS compounds and taking into account the calculation accuracy, we find the integral excess molar free energy of excess $\Delta_f G_T^{0,ex}$ of the $GaSe_{1-x}S_x$ solid solutions. Substituting the molar enthalpies and entropies of formation of the GaSe and GaS compounds, $\Delta C^0_{p,298.15}$, and $\Delta_f G_T^{0,ex}$ for the energy of mixing $\Delta_f G_T^{0,M}$ of the $GaSe_{1-x}S_x$ solid solutions in Eq. (2), we obtain

$$\Delta_f G_T^{0,M}(\text{GaSe}_{1-x}\text{S}_x) = x\left(4000 - 3000x^2\right) \times (1-x) + RT\left[x\ln(x) + (1-x)\ln(1-x)\right] \quad (4)$$

For thermodynamic description of the formation of $GaSe_{1-x}S_x$ solid solutions, it is sufficient to know the composition dependence of the excess molar free energy of mixing under isothermal conditions in the range 300–1200 K.

Using Eqs. (4), we calculated the free energies of mixing for the formation of $GaSe_{1-x}S_x$. The curves thus obtained are presented in Fig. 2 for the case calculated by Eq. (4) from thermodynamic data for the GaSe and GaS compounds.

As seen in Fig. 2, the sensitivity of the curve calculated for GaSe-GaS alloys by Eq. (4) is determined primarily by the entropy term. The curves obtained correspond to temperatures where the alloys are in crystalline and liquid states (300–1200 K). The $\Delta_f G_T^{0,M}(x)$ curve for $GaSe_{1-x}S_x$ at 800 K (curve *2*) is similar to that near the melting point of the alloys, 1200 K (curve *3*). Between 800 and 1200 K, there is a well-defined correlation with composition in the range 0 ≤ *x* ≤ 1. This suggests the formation of a thermodynamically stable $GaSe_{1-x}S_x$ configuration in this composition range.

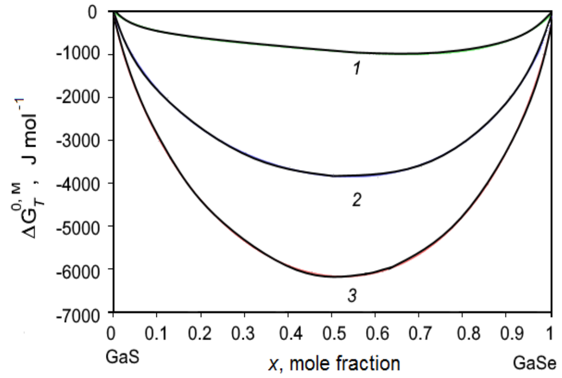

Fig. 2. Composition dependences of the Gibbs free energy of mixing calculated by Eq. (4) for $GaSe_{1-x}S_x$ solid solutions using data for GaSe and GaS: (*1*)300, (*2*)800, and (*3*)1200K.

Thus, it follows from thermodynamic analysis results that $GaSe_{1-x}S_x$ solid solutions have deviations from ideality. This is clearly seen in the composition and temperature dependences of the Gibbs free energy of mixing for $GaSe_{1-x}S_x$ in differential form, which demonstrate thermodynamic stability solid solution. According to thermodynamic theory, the formation of solid solutions is energetically favorable if $\Delta_f G_T^{0,M} \leq 0$. The above technique for evaluating the free energy of mixing of $GaSe_{1-x}S_x$ (Fig. 2) is consistent with this solution theory. As the temperature is varied, the free energy of mixing of alloys of the GaSe – GaS system assumes a negative value, which corresponds to solid solution formation.

The thermodynamic function of Gibbs mixing $\Delta_f G_T^{0,M}$ allows to assess the character and direction of molecular processes accompanying formation of $GaSe_{1-x}S_x$ solutions. The $\Delta_f G_T^{0,M}$ value is defined as the excess or the difference between real free energy and free energy for ideal solution. In other words, the excess free energy of mixing is non-ideal portion of the isobaric mixing potential.

The $\Delta_f G_T^{0,M}$ dependence of $GaSe_{1-x}S_x$ formation was calculated taking into account the experimental thermodynamic data for GaSe and GaS. For non-ideal $GaSe_{1-x}S_x$ solutions the additivity principle of excess free energy of mixing is not observed, and in calculations we took into account the entropy factor. Data on excess free energy of mixing allow to calculate the activity coefficients of components. As part of the regular solution theory, the partial free energy of mixing $\overline{G}^M$ is associated with activities (a_i) of components:

$$\overline{G}^M / RT = x_1 \ln a_1 + x_2 \ln a_2 = \\ = (1-x_2)\ln(1-x_2) + x_2 \ln x_2 + Kx_2(1-x_2) \quad ....(5)$$

K is parameter of regular solution, which is associated with excess Gibbs energy.

3.2.2. T-*x* phase diagrams of GaS–GaTe and GaSe–GaTe

Literature T-*x* and thermodynamic data for GaS–GaTe and GaSe–GaTe systems are shown in [8]. GaS–GaTe is a eutectic quasi-binary section. The eutectic contains 45 mol % GaTe at 1048 K. The GaS-based solubility is up to 2 mol % (α**) and GaTe-based solubility is up to 4 mol % (β**) in the GaSe–GaTe system.

GaSe–GaTe is a quasi-binary section. At 1:1 ratio of GaSe and GaTe, the intermediate Ga_2SeTe phase is detected and solid solutions based on it (γ). The compound Ga_2SeTe melting at 1120 K exists in this system. The eutectic coordinates are follows: 35 and 60 mol % GaTe and 1028 and 1038 K, respectively. The room-temperature solubility in GaSe is 10 mol % (α*); that in GaTe is 15 mol % (β*).

3 3. Isothermal section through the phase diagram of the GaSe–GaS–GaTe system

Formed in boundary systems GaSe-GaS, GaSe-GaTe and GaS-GaTe solid solutions and intermediate phase Ga_2SeTe, which has a homogeneity region γ are spread into concentration triangle. Not that the phase diagram of GaSe–GaS–GaTe given in [5] was built incorrectly. Phase fields in the isothermal section does not correspond to the Gibbs phase rule in adjoining areas. Three-phase areas must border with conodes. The correct version of phase equilibria in the solid state is represented by us below (Fig. 3).

3.4. Band gap of the GaSe–GaS system

Solid solutions have an important advantage over compounds, in particular because their band gap E_g can be varied. The $E_g(x)$ data for the $GaSe_{1-x}S_x$ solid solutions can be described by empirical equation with allowance for the deviation from additive behavior [9, 14].

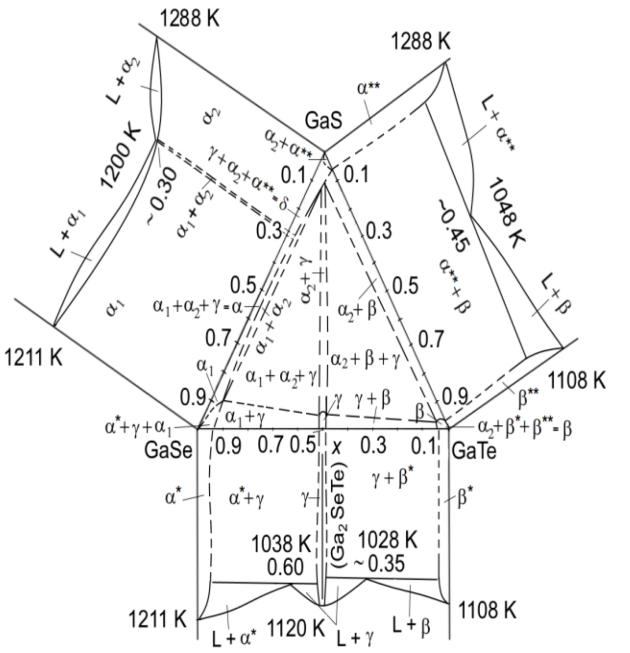

Fig. 3. 300-K isothermal section through the phase diagram of the GaSe–GaS–GaTe system. A solid solutions based (GaSe), δ solid solutions based (GaS), β solid solutions based (GaTe) and γ solid solutions based Ga_2SeTe. Triple phase Ga_2SeTe is formed on the GaSe-GaTe join.

The composition dependence of the band gap, $E_g(x)$, for $GaSe_{1-x}S_x$ was represented by the equation

$$E_g(x) = (1-x)E_g(\mathrm{GaSe}) + xE_g(\mathrm{GaS}) - bx(1-x) \quad \ldots(6)$$

where b quantifies the deviation from additivity.

The $E_g(x)$ data for the $GaSe_{1-x}S_x$ solid solutions are represented by a slightly concave curve, which means a negative deviation. Given that various E_g values have been reported for GaSe and GaS in the literature, we used average of b values for the deviation coefficient in Eq. (6).

Fig. 4 shows the 298-K $E_g(x)$ curves calculated for $GaSe_{1-x}S_x$ using Eq. (6) and average E_g values for GaSe and GaS.

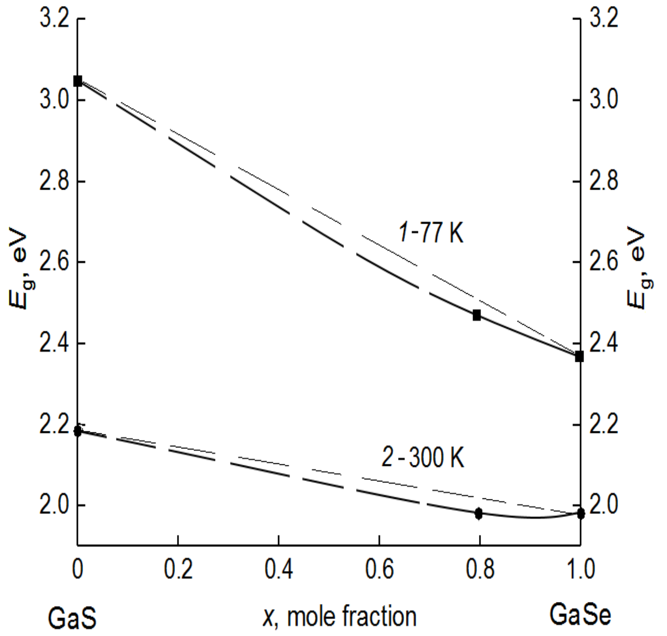

Fig. 4. Composition dependences of the 77-K (curves *1*) and 300-K (curves *2*) band gap calculated for $GaSe_{1-x}S_x$ solid solutions using Eq. (6).

The calculated $E_g(x)$ curves are in reasonable agreement also with our experimental data and data [1] for $GaSe_{1-x}S_x$ at low temperatures.

4 Conclusions

The quasi-ternary system GaSe–GaS–GaTe was re-investigated and the T–*x* phase diagram of GaSe–GaS was studied in detail by differential thermal analysis, X-ray diffractometry and thermodynamic calculations. We clarify the temperature and melting enthalpy of the components GaSe–GaS that are needed to calculate thermodynamic parameters. Thermodynamic parameters have been improved and adjusted to each other.

Equilibriums of melt and solid solutions $GaSe_{1-x}S_x$ have been thermodynamically described. In view of isothermal sections quasi-ternary system GaSe–GaS–GaTe is significantly affected by the phase boundary of the formation of solid solutions in the quasi-binary systems GaSe–GaS, GaS–GaTe, GaSe–GaTe. Isothermal section of system GaSe–GaS–GaTe at 300 K was built. Four phases of solid solutions based on α (GaSe), β(GaTe), δ(GaS), and γ (Ga_2SeTe) were found exhibiting maximum melting points at 1238, 1211, 1108 and 1123 K, respectively. We have synthesized and grew $GaSe_{1-x}S_x$ (x= 0, 0.2) single crystals with a hexagonal structure. Experiments show that in the prepared samples of solid solutions the concentration dependences of the properties are changed regularly.

References

[1] O. Madelung, Semiconductors Data Handbook. Springer-Verlag, Berlin. 2004.

[2] I.C.I. Terhell, Prog. *Cryst. Growth Charact. Mater.* 7, (1983) 55-110.

[3] S.N. Mustafaeva, M.M. Asadov, *Solid State Communications*, 45, (1983) 491-494.

[4] S.N. Mustafaeva, M.M. Asadov*, Materials Chemistry and Physics*, 15, (1986)185-189.

[5] I.A. Aliev, *Russian Journal of Inorganic Chemistry*, 53, (2008) 1795-1800.

[6] Y. Ni, H. Wu, C. Huang, M. Mao, Z. Wang, X. Cheng, *Journal of Crystal Growth*, 381, (2013) 10-14.

[7] M.M. Asadov, K.M. Ahmedly, *Inorganic Materials*, 32, (1996) 133-134.

[8] M.M. Asadov, K.M. Ahmedly, *Solid State Phenomena*, 138, (2008) 331-338.

[9] S.M. Asadov, A.N. Mamedov, S.A. Kulieva, *Inorganic Materials*, 52, (2016) 876-885.

[10] A.S. Abbasov, Termodinamicheskiye svoystva nekotorykh poluprovodnikovykh veshchestv (Thermodynamic properties of some semiconductor materials). Baku. Elm. 1981. (in Russian).

[11] V.P. Vasilev, *Inorganic Materials*, 43, (2007)115-124.

[12] A.V. Tyurin, K.S. Gavrichev, A.V. Khoroshilov, V.P. Zlomanov, *Inorganic Materials*, 50, (2014) 233-236.

[13] M. Ider, R. Pankajavalli, W. Zhuang, J.Y. Shen, T.J. Andersone, *ECS Journal of Solid State Science and Technology*, 4, (2015) Q51-Q60.

[14] K.W. Boer, Handbook of the Physics of Thin-Film Solar Cells. Springer Heidelberg New York Dordrecht London. 2013.